# Quantum correlations in $\mathcal{PT}$-symmetric systems

Quantum Science and Technology

PAPER

# Quantum correlations in $\mathcal{PT}$-symmetric systems

RECEIVED
24 September 2020

REVISED
12 November 2020

ACCEPTED FOR PUBLICATION
2 December 2020

PUBLISHED
22 January 2021

**Federico Roccati**[1,*], **Salvatore Lorenzo**[1], **G Massimo Palma**[1,2], **Gabriel T Landi**[3], **Matteo Brunelli**[4] **and Francesco Ciccarello**[1,2]

[1] Università degli Studi di Palermo, Dipartimento di Fisica e Chimica—Emilio Segrè, via Archirafi 36, I-90123 Palermo, Italy
[2] NEST, Istituto Nanoscienze-CNR, Piazza S. Silvestro 12, 56127 Pisa, Italy
[3] Instituto de Fısica, Universidade de Sao Paulo, CEP 05314-970, Sao Paulo, Sao Paulo, Brazil
[4] Cavendish Laboratory, University of Cambridge, Cambridge CB3 0HE, United Kingdom
[*] Author to whom any correspondence should be addressed.

**E-mail:** federico.roccati@unipa.it

**Keywords:** PT symmetry, quantum correlations, non-Hermitian, quantum discord

## Abstract

We study the dynamics of correlations in a paradigmatic setup to observe $\mathcal{PT}$-symmetric physics: a pair of coupled oscillators, one subject to a gain one to a loss. Starting from a coherent state, quantum correlations (QCs) are created, despite the system being driven only incoherently, and can survive indefinitely. Both total and QCs exhibit different scalings of their long-time behavior in the $\mathcal{PT}$-broken/unbroken phase and at the exceptional point (EP). In particular, $\mathcal{PT}$ symmetry breaking is accompanied by non-zero stationary QCs. This is analytically shown and quantitatively explained in terms of entropy balance. The EP in particular stands out as the most classical configuration, as classical correlations diverge while QCs vanish.

## 1. Introduction

The finding of non-Hermitian Hamiltonians with real eigenvalues [1] fueled widespread attention at a fundamental level, as well as in terms of potential applications [2–4]. A major motivation comes from the experimental implementability of such Hamiltonians, especially in optics [5–7]. A prototypical example (see figure 1) is a pair of coupled oscillators, separately subject to either gain or loss. At the mean-field level, the modes evolve according to a Schrödinger-like equation featuring a non-Hermitian Hamiltonian $\mathcal{H}$ that enjoys parity-time ($\mathcal{PT}$) symmetry [8].

To date the vast majority of studies of such dynamics adopted a classical description (based on Maxwell's equations in all-optical setups), thus neglecting quantum noise. Recent works yet showed that a full quantum treatment (beyond mean field) can have major consequences [9–12], although the exploration of this quantum regime is still in an early stage [13–23]. With regard to the potential exploitation of $\mathcal{PT}$-symmetric systems for quantum technologies, a major obstacle is that gain and loss unavoidably introduce quantum noise, which is detrimental for quantum coherent phenomena—entanglement above all [24]. In particular, the incoherent pumping due to the gain is unusual in quantum optics settings [25]. This issue even motivated recent proposals to employ parametric driving in place of gain/loss to effectively model non-Hermitian systems [12, 26].

Yet, in the last two decades, 'cheaper' quantum resources have been discovered that put milder constraints on the necessary amount of quantum coherence. Among these is quantum *discord*, a form of quantum correlations (QCs) that can occur even in absence of entanglement [27, 28]. This extended paradigm of QCs has received huge attention for its potential of providing a quantum advantage in noisy environments [29]. Remarkably, a very recent work reported the first experimental detection of such a form of QCs [30] in an anti-$\mathcal{PT}$-symmetric system featuring similarities with the setup in figure 1. However, whether or not QCs dynamics are sensitive to different $\mathcal{PT}$ symmetric phases is yet generally unknown.

This work puts forth a detailed study of total and quantum correlations in the case study of the gain-loss setup in figure 1, which is the simplest and most widely investigated system to implement $\mathcal{PT}$-symmetric non-Hermitian Hamiltonians [2]. We will show that, in addition to mean-field dynamics, $\mathcal{PT}$ symmetry


**Figure 1.** A pair of quantum oscillators $G$ and $L$ undergo a coherent exchange energy with rate $g$. Additionally, mode $G$ ($L$) is subject to a local gain (loss) with rate $\gamma$. The mean-field dynamics is described by a $\mathcal{PT}$-symmetric Hamiltonian. (Left): when $\mathcal{PT}$ symmetry is preserved ($g > \gamma$), if each mode starts in a coherent state (zero correlations), after some time they will share only classical correlations. (Right): $\mathcal{PT}$ symmetry breaking ($g < \gamma$) is instead accompanied by stationary quantum correlations.

breaking can be sensed by the long-time behavior of both total and QCs: these are found to display different scalings in the $\mathcal{PT}$-broken/unbroken phase and at the exceptional point (EP). This is proven analytically and the underlying mechanism explained in detail through entropic arguments. In particular, breaking of $\mathcal{PT}$ symmetry is accompanied by the appearance of finite stationary discord. Our study provides a new characterization of phases with unbroken/broken $\mathcal{PT}$ symmetry in terms of the asymptotic behavior of correlations, whose knowledge requires accounting for the full quantum nature of the field.

## 2. System

We consider two quantum harmonic oscillators $G$ and $L$ (see figure 1), whose joint state evolves in time according to the Lindblad master equation (we set $\hbar = 1$ throughout)

$$\dot{\rho} = -i[g(\hat{a}_L^\dagger \hat{a}_G + \text{H.c.}), \rho] + 2\gamma_L \mathcal{D}[\hat{a}_L]\rho + 2\gamma_G \mathcal{D}[\hat{a}_G^\dagger]\rho \tag{1}$$

with

$$\mathcal{D}[\hat{A}]\rho = \hat{A}\rho\hat{A}^\dagger - \frac{1}{2}(\hat{A}^\dagger\hat{A}\rho + \rho\hat{A}^\dagger\hat{A}).$$

Here, $\hat{a}_n$ and $\hat{a}_n^\dagger$ with $n = L, G$ are usual bosonic ladder operators $[\hat{a}_n, \hat{a}_n^\dagger] = 1$. Here, we assumed a rotating frame so as to eliminate the free Hamiltonian term $\omega_0(\hat{a}_G^\dagger \hat{a}_G + \hat{a}_L^\dagger \hat{a}_L)$, which does not affect any $G$–$L$ correlations. The coupling Hamiltonian in (1) describes a coherent energy exchange at rate $g$ between the two modes. In addition, each oscillator interacts incoherently with a local environment: the one on $G$ pumps energy with characteristic rate $\gamma_G$ (gain) while that on $L$ absorbs energy with rate $\gamma_L$ (loss). This system can be implemented in a variety of ways [2], including coupled waveguides [5], microcavities [7], inductively-coupled LRC circuits [31] and coupled pendula [32].

From equation (1) it follows that the evolution of the mean-field vector $\psi = (\langle \hat{a}_L \rangle, \langle \hat{a}_G \rangle)^{\mathrm{T}}$, with $\langle \hat{a}_L \rangle = \mathrm{Tr}\,(\hat{a}_L \rho)$ and similarly for $\langle \hat{a}_G \rangle$, is governed by the Schrödinger-like equation $i\dot{\psi} = \mathcal{H}\psi$ with

$$\mathcal{H} = \begin{pmatrix} -i\gamma_L & g \\ g & i\gamma_G \end{pmatrix}. \tag{2}$$

The non-Hermitian matrix $\mathcal{H}$ generally has two complex eigenvalues with associated non-orthogonal eigenstates. For $\gamma_L = \gamma_G = \gamma$ (the so-called '$\mathcal{PT}$ line'), $\mathcal{H}$ is invariant under $\mathcal{PT}$ symmetry, corresponding to a swap $G \leftrightarrow L$ combined with time reversal (complex conjugation). In this case, its eigenvalues are $\varepsilon_\pm = \pm\sqrt{g^2 - \gamma^2}$. These are real in the so called unbroken phase (UP) $\gamma < g$ and complex in the broken phase (BP) $\gamma > g$, coalescing at the EP $\gamma = g$ where the corresponding eigenstates become parallel [2]. Equations analogous to (1) for the full-quantum description of $\mathcal{PT}$-symmetric systems also appeared elsewhere (see e.g. references [33–35]).

## 3. Second-moment dynamics

The two oscillators have an associated quantum uncertainty described by a $4 \times 4$ covariance matrix. Introducing quadratures $\hat{x}_n = \frac{1}{\sqrt{2}}(\hat{a}_n + \hat{a}_n^\dagger)$ and $\hat{p}_n = \frac{i}{\sqrt{2}}(\hat{a}_n^\dagger - \hat{a}_n)$ (with $n = G, L$), we define the covariance matrix as $\sigma_{ij} = \langle \hat{X}_i \hat{X}_j + \hat{X}_j \hat{X}_i \rangle - 2\langle \hat{X}_i \rangle \langle \hat{X}_j \rangle$, where $\hat{X}_i = (\hat{x}_L, \hat{p}_L, \hat{x}_G, \hat{p}_G)$ [36]. Following a standard recipe [36], the master equation (1) implies a Lyapunov equation for the covariance matrix:

$$\dot{\sigma} = Y\sigma + \sigma Y^{\mathrm{T}} + 4D \tag{3}$$

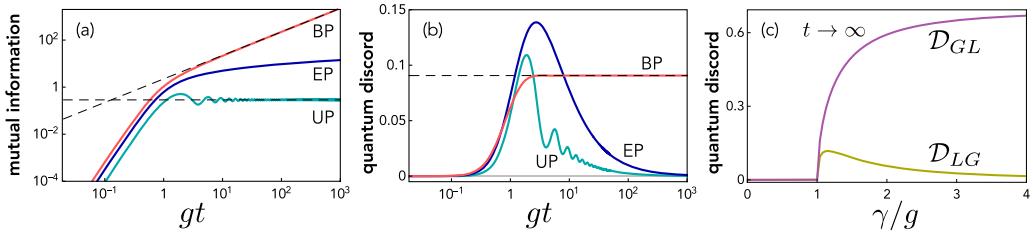


**Figure 2.** Evolution of total and quantum correlations on the $\mathcal{PT}$ line ($\gamma_L = \gamma_G = \gamma$). This comprises the UP $\gamma < g$, the EP $\gamma = g$ and the BP for $\gamma > g$. (a) and (b): mutual information $\mathcal{I}$ (a) and discord $\mathcal{D}_{LG}$ (b) for $\gamma = g/2$ (UP, green), $\gamma = 3g/2$ (BP, red) and $\gamma = g$ (EP, blue). A qualitatively analogous behavior is exhibited by $\mathcal{D}_{GL}$. (c): asymptotic value of discord, $\mathcal{D}_{LG}(\infty)$ (yellow) and $\mathcal{D}_{GL}(\infty)$ (purple). See appendix.

with

$$Y = \begin{pmatrix} -\gamma_L & 0 & 0 & g \\ 0 & -\gamma_L & -g & 0 \\ 0 & g & \gamma_G & 0 \\ -g & 0 & 0 & \gamma_G \end{pmatrix} \tag{4}$$

and $D = \frac{1}{2}\,\mathrm{diag}(\gamma_L, \gamma_L, \gamma_G, \gamma_G)$. The dynamics generated by equation (1) is Gaussian preserving, hence a Gaussian initial state will remain so at any time. Thereby, the entire state is fully specified by the mean-field vector $\psi$ and the covariance matrix $\sigma$ [37, 38].

## 4. Correlation measures

A measure of the *total* amount of correlations between modes $\hat{a}_G$ and $\hat{a}_L$ is given by the mutual information $\mathcal{I} = S_G + S_L - S$, which is the difference between the sum of local entropies $S_{L(G)} = -\mathrm{Tr}(\rho_{L(G)} \log \rho_{L(G)})$, with $\rho_{L(G)} = \mathrm{Tr}_{G(L)}\,\rho$, and the entropy of the joint system $S = -\mathrm{Tr}(\rho \log \rho)$ [24, 39]. This fulfills $\mathcal{I} = 0$ if and only if $\rho = \rho_L \otimes \rho_G$. Instead, the amount of QCs is measured by the so-called *quantum discord* [27–29]

$$\mathcal{D}_{LG} = S_G - S + \min_{\hat{G}_k} \sum_k p_k S(\rho_{L|k}), \tag{5}$$

where the minimization is over all possible quantum measurements $\{\hat{G}_k\}$ made on $G$. A measurement outcome indexed by $k$ collapses the joint system onto $\rho_{L|k} = \mathrm{Tr}_G(\hat{G}_k \rho)/p_k$ with probability $p_k$. Likewise, $\mathcal{D}_{GL}$ is obtained in terms of measurements on mode $L$ by swapping $G$ and $L$ in equation (5).

Note that discord is in general asymmetric, i.e., $\mathcal{D}_{LG} \neq \mathcal{D}_{GL}$, which is the typical case for our system [see figure 2(c)]. The difference $\mathcal{I} - \mathcal{D}_{LG}$ quantifies the maximum amount of information that can be extracted about $L$ only from local measurements on $G$. Based on this, discord captures QCs beyond entanglement, as it is in general nonzero for separable states [29]. Hence, correlations between the modes are wholly classical only when both $\mathcal{D}_{LG}$ and $\mathcal{D}_{GL}$ vanish but $\mathcal{I} \neq 0$.

For Gaussian states, the optimization in (5) can be restricted to Gaussian measurements (Gaussian discord) [40], leading to a closed-form, albeit cumbersome, expression for $\mathcal{D}$ [41, 42]. In order to provide a simpler analytic expression we replace the von Neumann entropy by the Rényi-2 entropy $S(\varrho) = -\log \mathrm{Tr}(\varrho^2)$ in each expression [43]. For Gaussian states, it has been shown that the choice of Rényi-2 entropy leads to well-behaved correlation measures [44]. We however numerically checked that all of the results presented (in particular asymptotic scalings to be discussed later) are qualitatively unaffected if von Neumann entropy is used instead. The fact that discord detects QCs more general than entanglement is condensed in a simple property: states such that $\mathcal{D} > \log 2$ are entangled ($\log 2 \to 1$ if von Neumann entropy is used) [42].

## 5. Correlations dynamics for balanced gain and loss

We study the dynamics of correlations when each oscillator $n = L, G$ starts in a coherent state $|\alpha_n\rangle = \mathrm{e}^{(\alpha \hat{a}_n^\dagger - \alpha^* \hat{a}_n)}|0\rangle$; the initial covariance matrix is thus simply $\sigma_0 = \mathbb{1}_4$ (note that this is independent of $\alpha_L$ and $\alpha_G$). We evolve the covariance matrix through equation (3) and then compute the time evolution of correlation measures $\mathcal{I}$, $\mathcal{D}_{LG}$ and $D_{GL}$ for which we obtain exact and compact expressions (see appendix). Instead, entanglement is zero at any time. It turns out that (5) admits a global minimum for all possible parameter values, which corresponds to a phase-insensitive (heterodyne) measurement. Intuitively, this

property can be traced back to the absence of any coherent drive: the dynamics in (1) preserves $U(1)$ symmetry and thus favors the conditioning of phase-insensitive measurements over phase-sensitive ones; this in turn makes the latter suboptimal for generating QCs.

Figure 2, where we set $\gamma_L = \gamma_G = \gamma$ ($\mathcal{PT}$ line), shows the typical time behavior of mutual information $\mathcal{I}$ (a) and discord $\mathcal{D}$ (b) in the UP (green line), at the EP (blue) and in the BP (red). Correlations, including QCs, are created on a typical time scale (transient time) of the order of $\sim g^{-1}$ or less (see appendix for details). As discussed later on, *transient* generation of QCs is common in noise-driven multipartite systems. In the long-time limit, instead, correlations show a peculiar behavior, which we next analyze for each phase (namely in the UP, BP and at the EP).

In the UP, $\mathcal{I}$ saturates to a finite value and exhibits secondary oscillations at frequency $2\sqrt{g^2-\gamma^2}$, while discord slowly decays until it vanishes. Their asymptotic expressions are given by (see appendix for details)

$$\mathcal{I} \approx \log\left(\frac{g^2}{g^2-\gamma^2}\right), \qquad \mathcal{D}_{LG}, \mathcal{D}_{GL} \approx \frac{\gamma}{2g^2 t}, \tag{6}$$

showing that discord undergoes a power-law decay in this phase (throughout the symbol $\approx$ indicates the long-time limit). Thus in the UP asymptotic correlations are *entirely classical*, i.e., they do not involve any quantum superposition. At a glance, this may seem to contradict the well-known property that Gaussian states such that $\mathcal{I} = 0$ are all and only those with zero discord [42]. That property yet holds for systems with bounded mean energy, while the present dynamics is *unstable* on the whole $\mathcal{PT}$ line (see appendix for details).

When $\mathcal{PT}$ symmetry is broken, on the other hand, the behavior of long-time correlations changes dramatically. The mutual information now grows linearly as $\mathcal{I} \approx 2\Omega\, t$, with $\Omega = \sqrt{\gamma^2 - g^2}$, while QCs tend to a finite value given by

$$\mathcal{D}_{LG} \approx \log\left(\frac{\gamma(\gamma+\Omega)+g^2}{2\gamma^2}\right), \quad \mathcal{D}_{GL} \approx \log\left(\frac{\gamma(3\gamma+\Omega)-g^2}{2\gamma^2}\right). \tag{7}$$

Thus in the BP *stationary* QCs are established, notwithstanding the noisy action of gain/loss and despite the dynamics being unstable.

Jointly taken, equations (6) and (7) show that the nature of long-time correlations is different in the two phases. In each phase, stationary finite correlations occur, but these are purely classical in the UP (where $\mathcal{I}$ converges, while $\mathcal{D} \to 0$) and quantum in the BP.

Finally, a special behavior occurs at the EP with the correlations scaling as

$$\mathcal{I} \approx \log\left(\frac{4g^2}{3}t^2\right), \quad \mathcal{D}_{LG}, \mathcal{D}_{GL} \approx \frac{1}{gt}. \tag{8}$$

Thus, while discord scales as in the UP phase (although with a different pre-factor, cf (6)), the growth of mutual information is now logarithmic. Notably, the EP is the only point on the $\mathcal{PT}$ line such that $\mathcal{I} \to \infty$, $\mathcal{D} \to 0$ (purely classical and diverging correlations). Thus, for balanced gain and loss, the EP can be regarded as the *most classical* configuration.

Figure 2(c) shows the stationary QCs on the $\mathcal{PT}$ line. In the BP, $\mathcal{D}_{GL}(\infty)$ monotonically grows with $\gamma$ asymptotically approaching the entanglement threshold, while $\mathcal{D}_{LG}(\infty)$ takes a maximum followed by a long-tail decay. A critical behavior occurs at the EP (on the boundary between regions of zero and non-zero discord) since $\mathcal{D} \sim (\gamma/g - 1)^{\frac{1}{2}}$ for $\gamma > g$ while $\mathcal{D} = 0$ for $\gamma \leqslant g$.

As specified previously, all the plots in figure 2 are for an initial coherent state. Yet, we gathered numerical evidence that different initial Gaussian states yield analogous long-time behaviors of correlations (see appendix).

## 6. Dynamics of correlations beyond the PT line

We next address the rich dynamics of correlations beyond the $\mathcal{PT}$ line, i.e., for unbalanced gain and loss ($\gamma_L \neq \gamma_G$). The phase portrait in figure 3 displays five distinct dynamical regimes, obtained by applying standard stability analysis (see appendix for details). These regions are limited by the $\mathcal{PT}$ line, the EP line $\gamma_L + \gamma_G = 2g$ and the hyperbola $\gamma_L\gamma_G = g^2$. There is a stable region (III + IV), where both distinct eigenvalues $\lambda_\pm$ of matrix $Y$ (cf (4)) have negative real part (note that for $g > \gamma_G$ a too large rate $\gamma_L$ makes the dynamics unstable). This is the usual bounded-energy region featuring non-zero stationary values of $\mathcal{I}$ and $\mathcal{D}$. Symmetric to that is a totally unstable region (I + II), where both $\Re\lambda_\pm > 0$. Notably, this *whole* region is characterized by asymptotically vanishing discord [cf figure 3(c)]. The EP line separates two kinds of divergence (convergence) in the totally unstable (stable) region: below this line there occur repulsive

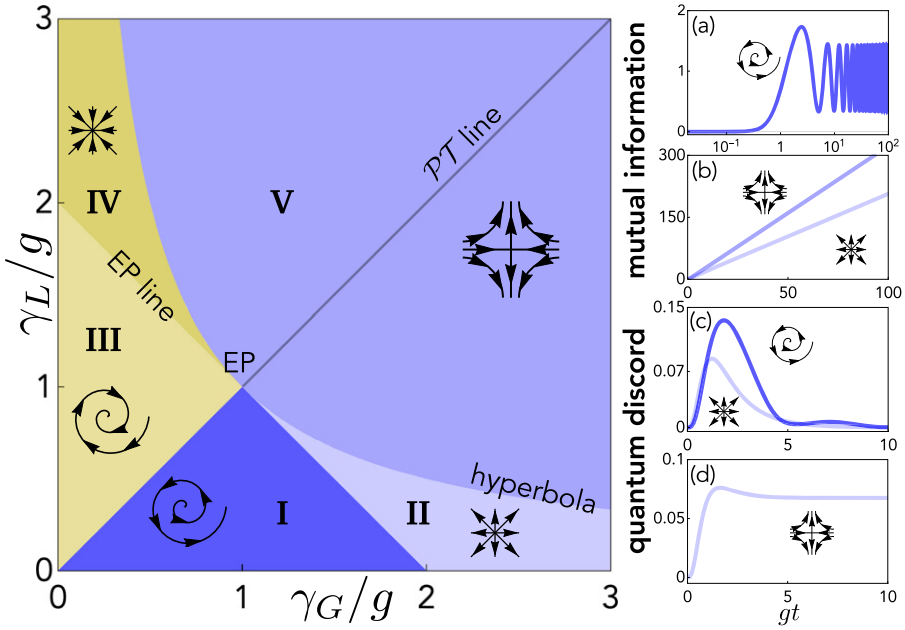


**Figure 3.** (Left): stability diagram for the dynamics ruled by (1) with unbalanced ga in and loss; see text for details. (Right): typical time evolution of the mutual information [(a), (b)] and discord [(c), (d)] corresponding to the points highlighted in the diagram. Asymptotic discord vanishes in the I + II region and along the line $\gamma_G = 0$.

(attractive) spirals, and sources (sinks) above it. Finally, there is an unstable region (V) (saddle points) with linearly divergent $\mathcal{I}$ and stationary QCs [cf (b) and (d)]. Yet another remarkable feature is that the region (I + III + IV) is characterized by asymptotic finite values of $\mathcal{I}$. In particular, in region I, $\mathcal{I}$ displays extremely long-lived oscillations [see figure 3(a)].

## 7. Physical mechanisms behind generation of correlations

Generation of QCs during the *transient* dynamics can be understood by noting that the coupling Hamiltonian acts on the modes like a beam splitter. When acting on $|\alpha_L\rangle \otimes |\alpha_G\rangle$, the coupling Hamiltonian alone cannot correlate the modes, but only mix their amplitudes [45]. Thus $|\alpha_L\rangle \otimes |\alpha_G\rangle \to |\tilde{\alpha}_L\rangle \otimes |\tilde{\alpha}_G\rangle$ where $\tilde{\alpha}_{L(G)}$ is a linear combination of $\alpha_L$ and $\alpha_G$. The loss term of course does not correlate either, its action being described by $|\alpha_L\rangle \otimes |\alpha_G\rangle \to |\eta\alpha_L\rangle \otimes |\alpha_G\rangle$ with $0 \leqslant \eta < 1$. The gain, on the other hand, turns a coherent state of $G$ into a *mixture*, namely

$$|\alpha_G\rangle\langle\alpha_G| \to \int \mathrm{d}^2\alpha'_G\, P(\alpha'_G)|\alpha'_G\rangle\langle\alpha'_G| \tag{9}$$

with $P(\alpha'_G) \geqslant 0$, that is a state with reduced coherence [46].

Overall, the combined action of beam splitter, loss and gain transforms the initial state as

$$|\alpha_L\rangle\langle\alpha_L| \otimes |\alpha_G\rangle\langle\alpha_G| \to \int \mathrm{d}^2\alpha\, P(\alpha)|\alpha_L(\alpha)\rangle\langle\alpha_L(\alpha)| \otimes |\alpha_G(\alpha)\rangle\langle\alpha_G(\alpha)|. \tag{10}$$

Although disentangled, one such correlated state is generally discordant because coherent states form a *non*-orthogonal basis [47]. We note that a similar effect is obtained if the gain is replaced by a local thermal bath. Indeed, the ability of certain local non-unitary channels to favor creation of discord was demonstrated in [29]. For instance, local gain or loss can create QCs starting from a state featuring only classical correlations (a process which is not possible for entanglement) [48–51], which was experimentally confirmed in reference [52].

The peculiar nature of the present dynamics mostly comes from the *long-time* behavior of correlations. To shed light on it, we first express the discord in the form

$$\mathcal{D}_{LG} = \log\left(1 + \frac{\mathrm{e}^{\mathcal{I}} - 1}{\mathrm{e}^{S_G} + 1}\right), \tag{11}$$

(with an analogous expression for $L \leftrightarrow G$). This identity, which is proven in the appendix, holds true for *any* Gaussian state generated by (1) and subject to a local heterodyne measurement. Notably, at variance

**Table 1.** Asymptotic behavior of $S$ and $S_{L(G)}$ on the $\mathcal{PT}$ line.

| $\mathcal{PT}$ line | UP | EP | BP |
|---|---|---|---|
| $S$ | $\log\left(\frac{4\gamma^2 g^2}{g^2-\gamma^2}t^2\right)$ | $\log\left(\frac{4g^4}{3}t^4\right)$ | $2\Omega t+\log\left(\frac{\gamma^3(\gamma+\Omega)}{\Omega^4}\right)$ |
| $S_L$ | $\log\left(\frac{2\gamma g^2}{g^2-\gamma^2}t\right)$ | $\log\left(\frac{4g^3}{3}t^3\right)$ | $2\Omega t+\log\left(\frac{\gamma g^2}{2\Omega^3}\right)$ |
| $S_G$ | | | $2\Omega t+\log\left(\frac{\gamma(\gamma+\Omega)^2}{2\Omega^3}\right)$ |

with (5), equation (11) no longer features any optimization to be performed, but instead expresses discord as an explicit function of mutual information and local entropy.

Combined with $\mathcal{I}=S_G+S_L-S$, equation (11) allows to explain the dynamics of classical and QCs in terms of a *competition* between global and local entropies. This task is relatively straightforward on the $\mathcal{PT}$ line, in which case the long-time expressions of $S$ and $S_{L(G)}$ are reported in table 1. All of these *diverge* in time (either logarithmically or linearly depending on the phase). Hence, (11) simplifies to

$$\mathcal{D}_{LG}\approx\log\left(1+\mathrm{e}^{-(S-S_L)}-\mathrm{e}^{-S_G}\right), \tag{12}$$

which shows that the survival of QCs is controlled by $S-S_L$ alone. Using the expressions in table 1 and (12) yields precisely the scalings in equations (6), (7) and (8).

In the UP, $S_G$ and $S_L$ grow at the same rate and their sum is *almost* equal to the global entropy $S$. Their difference is small (showing this requires sub-leading contributions not reported in table 1) and yields constant $\mathcal{I}$ in the long-time limit. Equation (11) then entails that discord vanishes. In the BP, instead, the gain dominates the entropy balance (i.e., $S_G>S_L$) and the total entropy is slaved to the local one, $S\approx S_G$. This in turn implies $\mathcal{I}\approx S_L$. Moreover, the divergences of $S$ and $S_L$ cancel out, so that $S-S_L$ is convergent, in turn entailing a finite value of QCs via (12).

The above reasoning concerns the $\mathcal{PT}$ line $\gamma_L=\gamma_G=g$. Analogous arguments can be developed on any line $\gamma_L=\beta\gamma_G$ with $\beta<1$, where however the expressions of global and local entropies are not as compact as those in table 1. The transition between the two different scalings now occurs at point $\gamma_G=\frac{1}{\sqrt{\beta}}g$, $\gamma_L=\sqrt{\beta}g$.

The fact that both mean field and correlations can exhibit a transition between different regimes corresponding to the same parameters is due to the form of matrix $Y$ entering the second-moment dynamics in equation (3). Indeed, it is easily shown (see appendix) that, under a suitable canonical transformation, $Y$ takes the form

$$Y=\begin{pmatrix}-i\mathcal{H} & \mathbf{0}\\ \mathbf{0} & i\mathcal{H}^\dagger\end{pmatrix}. \tag{13}$$

The eigenvalues of $Y$ are thus the same as those of matrix $-i\mathcal{H}$ [see equation (2)] with a double degeneracy. This property is a consequence of the form of the Lindblad master equation (1) (in particular the beam-splitter-like interaction between the modes) and holds even for setups with more than two modes (obeying a master equation of the same type) [53].

Lastly, we comment on the fact that zero discord can occur without a simultaneous vanishing of mutual information. As mentioned previously, any two-mode Gaussian state with finite mean energy fulfills $\mathcal{D}\neq 0\Leftrightarrow\mathcal{I}\neq 0$ [42]. This property can be retrieved from (11) when $S_G$ is *finite*. Yet, for $S_G\to\infty$, discord can vanish asymptotically even if $\mathcal{I}$ does not (e.g. in the UP and at EP, see figure 2).

## 8. Conclusions

Through a fully quantum description, we studied the dynamics of total and quantum correlations in a typical gain-loss system exhibiting $\mathcal{PT}$-symmetric physics. With the modes initially in a coherent state, QCs without entanglement are created and, in a large region of the parameter space, settle to a non-zero value. For balanced gain and loss, in particular, and in the long-time limit, phases with distinct $\mathcal{PT}$ symmetry exhibit dramatically different time scalings of both total and quantum correlations. This suggests a new distinction between phases with unbroken/broken $\mathcal{PT}$ symmetry in the dynamics of entropic quantities, whose knowledge requires accounting for the full quantum nature of the field.

From the viewpoint of QCs theory, the unstable nature of the dynamics brings about exotic behaviors such as diverging correlations of a purely classical nature, which arise at the exceptional point.

In terms of quantum technologies, stationary QCs beyond entanglement (occurring e.g. in the unbroken phase) are potentially appealing in that this form of correlations have found several applications in recent years, [54, 55] such as information encoding [56], remote-state preparation [57], entanglement activation

[58–61], entanglement distribution [62–65], quantum metrology and sensing [66] and so on. This suggests that quantum noise could embody a resource, rather than a hindrance, to the exploitation of $\mathcal{PT}$-symmetric systems for useful applications. Future important tasks will be studying the effect of finite temperature and gain saturation (the latter introduces non-linearities affecting the Gaussian nature of the dynamics).

## Acknowledgments

We acknowledge fruitful discussions with M Paternostro, V Giovannetti, P Rabl, and T Tufarelli. FR acknowledges partial support from GNFM-INdAM. GMP, FC and SL acknowledge PRIN Project No. 2017 SRN-BRK QUSHIP funded by MIUR. GTL acknowledges the University of Palermo, for both the hospitality and the financial support. MB acknowledges support by the European Union Horizon 2020 research and innovation program under Grant Agreement No. 732894 (FET Proactive HOT).

## Appendix A. Covariance matrix and correlations

On the $\mathcal{PT}$ line excluding the EP, that is for $\gamma_L = \gamma_G = \gamma \neq g$, the solution of equation (3) in the main text under the initial condition $\sigma(0) = \mathbb{1}_4$ (product of coherent states) reads

$$\sigma_{11}(t) = \sigma_{22}(t) = \frac{\gamma g^2 \sinh(2\Omega t)}{\Omega^3} - \frac{2\gamma g^2 t}{\Omega^2} + 1$$

$$\sigma_{14}(t) = -\sigma_{23}(t) = -\frac{\gamma g}{\Omega^2} + \frac{\gamma^2 g \sinh(2t\Omega)}{\Omega^3} - \frac{2\gamma^2 g t}{\Omega^2} + \frac{\gamma g \cosh(2t\Omega)}{\Omega^2},$$

$$\sigma_{33}(t) = \sigma_{44}(t) = -\frac{\gamma^2 + 2\gamma g^2 t + g^2}{\Omega^2} + \frac{2\gamma^2 \cosh(2t\Omega)}{\Omega^2} + \frac{\gamma\left(\gamma^2 + \Omega^2\right)\sinh(2t\Omega)}{\Omega^3},$$

where $\Omega = \sqrt{\gamma^2 - g^2}$ and all the remaining matrix entries vanish. In unbroken phase, $\Omega = i\sqrt{g^2 - \gamma^2}$ and hyperbolic functions are turned into oscillating functions of $\sqrt{g^2 - \gamma^2}\, t$. At the EP $\gamma = g$ the solution reads

$$\sigma_{11}(t) = \sigma_{22}(t) = \frac{4g^3t^3}{3} + 1, \quad \sigma_{33}(t) = \sigma_{44}(t) = \frac{4g^3t^3}{3} + 4g^2t^2 + 4gt + 1,$$

$$\sigma_{14}(t) = -\sigma_{23}(t) = \frac{4g^3t^3}{3} + 2g^2t^2,$$

with all the remaining matrix entries being zero. Although exact analytical solution of equation (3) outside of the $\mathcal{PT}$ line can be found, their expressions are not reported here since these are lengthy and uninformative.

Mean energy of joint and reduced states can be easily computed from the covariance matrix as $E = \operatorname{Tr}\sigma$ and $E_{L(G)} = \operatorname{Tr}\sigma_{L(G)}$, respectively. On the $\mathcal{PT}$ line and in the long-time limit, they scale as $E_{\mathrm{UP}}(t) \approx \frac{8g^2\gamma}{g^2-\gamma^2}\, t$, $E_{L,\mathrm{UP}}(t) \approx \frac{1}{2} E_{\mathrm{UP}}(t)$, $E_{\mathrm{EP}}(t) \approx \frac{16g^3}{3} t^3$, $E_{L,\mathrm{EP}}(t) \approx \frac{1}{2} E_{\mathrm{EP}}(t)$ and $E_{\mathrm{BP}}(t) \approx \frac{2\gamma^2(\gamma+\Omega)}{\Omega^3}\, \mathrm{e}^{2\Omega t}$, $E_{L,\mathrm{BP}}(t) \approx \frac{g^2\gamma}{2\gamma^2(\gamma+\Omega)} E_{\mathrm{BP}}(t)$.The general form of $\sigma$ generated by equation (1) with an initial product of coherent state features $2 \times 2$ blocks

$$\sigma = \begin{pmatrix} L & C \\ C^{\mathrm{T}} & G \end{pmatrix}, \tag{A.1}$$

where $L = \mathrm{diag}(\sigma_{11}, \sigma_{22})$, $G = \mathrm{diag}(\sigma_{33}, \sigma_{44})$ and $C = \begin{pmatrix} 0 & \sigma_{14} \\ \sigma_{23} & 0 \end{pmatrix}$ describe uncertainties affecting the local fields $L$ and $G$ and cross-correlations, respectively.

### A.1. Total and local entropies

The knowledge of the covariance matrix allows to work out all entropic quantities. Such task is particularly simple using the Rényi-2 entropy. This is because, while von Neumann entropy requires the knowledge of the symplectic eigenvalues of $\sigma$, the Rényi-2 entropy for Gaussian states is simply given by

$$S(\sigma) = \frac{1}{2} \ln |\sigma|, \tag{A.2}$$

with $|\sigma| \equiv \det(\sigma)$. The entropies of the reduced states of $L$ and $G$ (local entropies) are similarly obtained as $S(L)$ and $S(G)$. Plugging in the expressions for $\sigma_{ij}$ then leads to the results in table 1 of the main text.

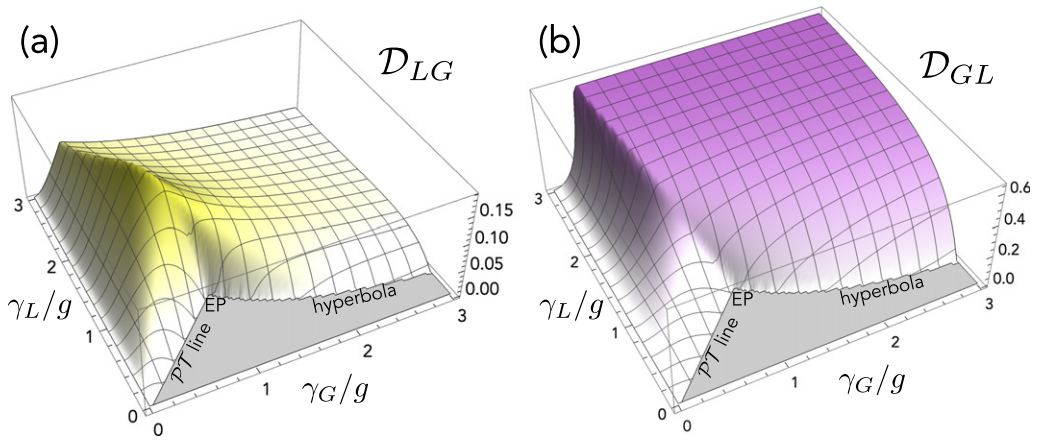


**Figure B1.** Long time QCs as measured by $\mathcal{D}_{LG}$ (a) and $\mathcal{D}_{GL}$ (b) on the plane $\gamma_G - \gamma_L$ (in units of $g$). $\mathcal{PT}$ line, EP and hyperbola are highlighted to clarify the relation with figure 3 in the main text.

## Appendix B. Analytical expressions for discord

Despite a closed expression for bipartite Gaussian quantum discord can be obtained, it is generally lengthy and uninformative regardless of the chosen entropy measure. However, in our dynamics with initial product of coherent states, the isotropy of the problem suggests that the measurement which maximizes discord is likely to be phase-insensitive. Indeed, it can be checked that heterodyne detection (i.e., projection onto coherent states) is the optimal measurement. In our dynamics it can also be checked that cross correlations are always smaller than local uncertainties (this is of course not true for *any* Gaussian state). These facts allow us to write quantum discord as in equation (9) according to the following lemma.Using (B.1) we plot asymptotic discord in figure B1.

**Lemma.** *For a heterodyne measurement Gaussian discord with Rényi-2 entropy of a Gaussian state as in equation (A.1) whose cross correlations are smaller than local uncertainties (i.e.,* $|C| < \sqrt{|L|}\sqrt{|G|}$*) can be written as*

$$\mathcal{D}_{LG} = \log\left(1 + \frac{\mathrm{e}^{\mathcal{I}} - 1}{\mathrm{e}^{S_G} + 1}\right), \qquad \mathcal{D}_{GL} = \log\left(1 + \frac{\mathrm{e}^{\mathcal{I}} - 1}{\mathrm{e}^{S_L} + 1}\right). \tag{B.1}$$

**Proof.** A heterodyne measurement on $G$ turns the CM into $\sigma_{|G} = \begin{pmatrix} L & C \\ C^T & G + \sigma_M, \end{pmatrix}$, where $\sigma_M = \mathbb{1}_2$ is the CM of the measurement outcome [38]. Let $\tilde{L} = L - C(G + \sigma_M)^{-1}C^{\mathrm{T}}$ be the Schur complement and let us denote $|A| \equiv \det(A)$. Using the definition of Gaussian discord with Rényi-2 entropy [43] $\mathcal{D}_{LG} = \frac{1}{2}\log\left(\frac{|\tilde{L}||G|}{|\sigma|}\right)$ we get

$$\mathcal{D}_{LG} = \frac{1}{2}\log\left(\frac{|G|}{|G+\sigma_M|}\frac{|G+\sigma_M||\tilde{L}|}{|\sigma|}\right) = \frac{1}{2}\log\left(\frac{|G|}{|G+\sigma_M|}\frac{|\sigma_{|G}|}{|\sigma|}\right).$$

Now using the assumption $|C| < \sqrt{|L|}\sqrt{|G|}$ we can write

$$\mathcal{D}_{LG} = \frac{1}{2}\log\left(\frac{\mathrm{e}^{2S_G}}{(\mathrm{e}^{S_G}+1)^2}\frac{(\mathrm{e}^{S} + \mathrm{e}^{S_L})^2}{\mathrm{e}^{2S}}\right) = \log\left(1 + \frac{\mathrm{e}^{\mathcal{I}} - 1}{\mathrm{e}^{S_G} + 1}\right).$$

Analogous proof holds for $\mathcal{D}_{GL}$.

## Appendix C. Absence of entanglement

As mentioned in the main text, discord detects QCs more general than entanglement. For Gaussian discord, this is condensed in a simple property: Gaussian states such that $\mathcal{D} > \log 2$ (1 with von Neumann entropy) are entangled. In our setup, discord never exceeds this threshold (see figure 2(c)) and we checked that the state is never entangled as $\tilde{\nu}_- > 1$ at any time ($\tilde{\nu}_-$ is the smallest symplectic eigenvalue of the partially transposed CM [42]). Besides these analytical results, absence of entanglement at any given time is justified by the fact that the coupling Hamiltonian acts like a beam-splitter, and cannot therefore entangle coherent states, and that the two gain/loss channels are local.

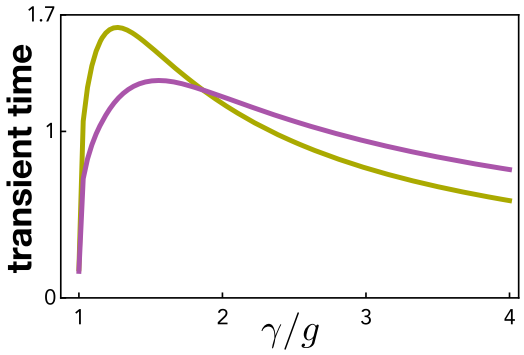


**Figure E1.** Transient time $\tau_{LG}$ (yellow) and $\tau_{GL}$ (purple) in units of $g^{-1}$ versus gain/loss rate $\gamma$ in units of $g$.

## Appendix D. Stability analysis

Schrödinger-like equation for the mean-field $\dot{\psi} = -i\mathcal{H}\psi$ is nothing but a two dimensional linear dynamical system whose asymptotic behavior is completely characterized by the eigenvalues $\lambda_\pm = \frac{1}{2}(\gamma_G - \gamma_L \pm \sqrt{(\gamma_G + \gamma_L)^2 - 4g^2})$ of $-i\mathcal{H}$. If $\lambda_+\lambda_- < 0$ then the origin $O = (0, 0)$ is a saddle point for the dynamical system. If both $\lambda_\pm$ are real numbers then $O$ is a source (sink) if both $\lambda_\pm > 0$ ($\lambda_\pm < 0$), otherwise $O$ is a repulsive (attractive) spiral if both $\Re\lambda_\pm > 0$ ($\Re\lambda_\pm < 0$). The boundaries separating regions with different behaviors are exactly the $\mathcal{PT}$ line ($\gamma_L = \gamma_G < g$), the hyperbola ($\gamma_L\gamma_G = g^2$) and the EP line ($\gamma_L + \gamma_G = 2g$), as shown in figure 3.

Accordingly, the asymptotic behavior of the CM is determined by the Lyapunov stability criterion: equation $Y\sigma_\infty + \sigma_\infty Y^{\mathrm{T}} + 4D = 0$ has a (finite) solution if and only if the eigenvalues of $Y$ have negative real parts. We observe that, by expressing the CM in terms of ladder operators $\hat{X}_i = (\hat{a}_L, \hat{a}_G, \hat{a}_L^\dagger, \hat{a}_G^\dagger)$ (instead of quadratures as in the main text), matrix $Y$ entering equation (4) turns into $\widetilde{Y} = \begin{pmatrix} -i\mathcal{H} & \mathbf{0} \\ \mathbf{0} & i\mathcal{H}^\dagger \end{pmatrix}$. The eigenvalues of $Y$ are thus same as those of $\widetilde{Y}$ (as a unitary transformation preserves the spectrum) and are in turn the same as those of matrix $-i\mathcal{H}$ with a double degeneracy. Therefore CM dynamics mimics that of the Schrödinger-like equation for the mean-field: it admits a stationary value for $\Re\lambda_\pm < 0$ [regions III + IV in figure 3], otherwise it diverges.

## Appendix E. Transient time

Stationary QCs occur only when the dynamics is unstable. It is therefore important from an experimental point of view to compute the transient time $\tau$, namely the time it takes for QCs to reach a relevant percentage of their asymptotic value. We focus here on the $\mathcal{PT}$ line in broken phase and define $\tau_{LG}$ as that time satisfying $\mathcal{D}_{LG}(\tau_{LG}) = 90\%\,\mathcal{D}_{LG}(\infty)$, with an analogous definition for $\tau_{GL}$. From figure E1, we see that both $\tau$'s are of the order of $g^{-1}$. We numerically checked that this holds true besides the $\mathcal{PT}$-broken phase whenever asymptotic discord is finite.

## Appendix F. Other initial states

All the results and plots in the main text are for an initial coherent state (covariance matrix $\sigma_0 = \mathbb{1}_4$). Yet, we gathered numerical evidence that mutual information and discord exhibit analogous long-time behaviors if different (Gaussian) initial states are chosen. This is illustrated in figure F1 where we set $\gamma_G = \gamma_L = \gamma$ ($\mathcal{PT}$ line) and plot mutual information and $\mathcal{D}_{GL}$ versus time for three different choices of initial state: a coherent state, a two-mode squeezed state and a two-mode squeezed thermal state, whose general covariance matrix (in quadrature basis) has the form

$$\sigma_0 = \begin{pmatrix} (\cosh r\,(n_G + n_L + 1) + n_L - n_G)\mathbb{1}_2 & \sinh\,(n_G + n_L + 1)\,\sigma_z \\ \sinh\,r\,(n_G + n_L + 1)\,\sigma_z & (\cosh\,r\,(n_G + n_L + 1) + n_G - n_L)\mathbb{1}_2 \end{pmatrix} \tag{F.1}$$

where $\sigma_z = \begin{pmatrix} 1 & 0 \\ 0 & -1 \end{pmatrix}$, $r$ is the squeezing parameter and $n_L(n_G)$ is the mean number of photons in mode $L(G)$. Note that changing the initial states does not even affect the numerical asymptotic value except for the

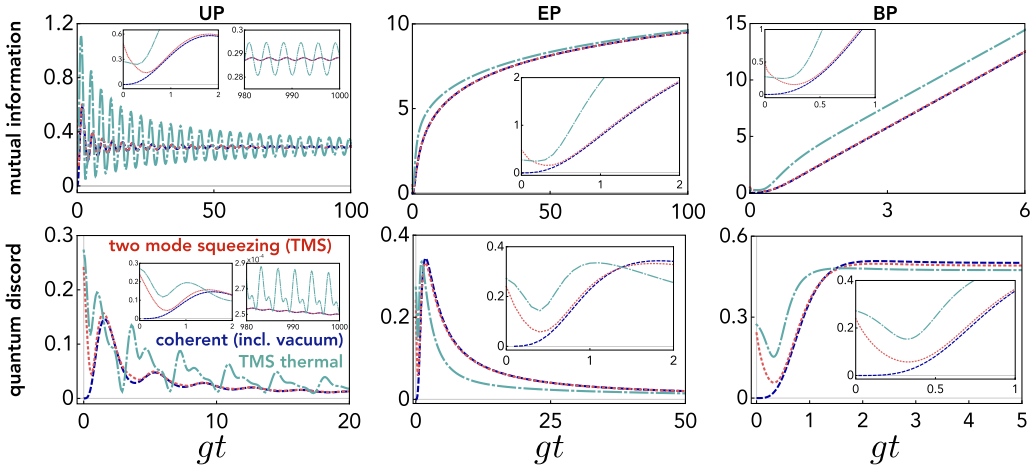


**Figure F1.** Typical time behavior on the $\mathcal{PT}$ line of mutual information (top panels) and discord $\mathcal{D}_{GL}$ (bottom) for different choices of the initial state as in (F.1): coherent (blue, $r = 0$, $n_L = n_G = 0$), two mode squeezed (red, $r = 0.5$, $n_L = n_G = 0$) and two mode squeezed thermal (green, $r = 0.5$, $n_L = 3$, $n_G = 7$) state. The three columns represent UP ($\gamma = g/2$), EP ($\gamma = g$) and BP ($\gamma = 3g/2$).

BP where a little discrepancy between different initial states arises. We checked that this discrepancy disappears if Von Neumann entropy is used instead of Rényi-2 entropy.

## ORCID iDs

Federico Roccati https://orcid.org/0000-0002-6981-0613
Salvatore Lorenzo https://orcid.org/0000-0002-0827-5549
G Massimo Palma https://orcid.org/0000-0001-7009-4573
Gabriel T Landi https://orcid.org/0000-0001-8451-9712
Matteo Brunelli https://orcid.org/0000-0002-5023-3780
Francesco Ciccarello https://orcid.org/0000-0002-6061-1255

## References

[1] Bender C M and Boettcher S 1998 Real spectra in non-Hermitian Hamiltonians having PT symmetry$\mathcal{PT}$ symmetry *Phys. Rev. Lett.* **80** 5243–6
[2] El-Ganainy R, Makris K G, Khajavikhan M, Musslimani Z H, Rotter S and Christodoulides D N 2018 Non-Hermitian physics and PT symmetry *Nat. Phys.* **14** 11–9
[3] Liang F, El-Ganainy R and Ge L 2017 Non-Hermitian photonics based on parity–time symmetry *Nat. Photon.* **11** 752
[4] Longhi S 2017 Parity-time symmetry meets photonics: a new twist in non-Hermitian optics *Europhys. Lett.* **120** 64001
[5] Rüter C E, Makris K G, El-Ganainy R, Christodoulides D N, Segev M and Kip D 2010 Observation of parity-time symmetry in optics *Nat. Phys.* **6** 192–5
[6] Regensburger A, Bersch C, Miri M-A, Onishchukov G, Christodoulides D N and Peschel U 2012 Parity-time synthetic photonic lattices *Nature* **488** 167–71
[7] Peng B 2014 Parity-time-symmetric whispering-gallery microcavities *Nat. Phys.* **10** 394–8
[8] Bender C M and Mannheim P D 2010 Symmetry and necessary and sufficient conditions for the reality of energy eigenvalues *Phys. Lett.* A **374** 1616–20
[9] Kepesidis K V, Milburn T J, Huber J, Makris K G, Rotter S and Rabl P 2016 $\mathcal{PT}$-symmetry breaking in the steady state of microscopic gain–loss systems *New J. Phys.* **18** 095003
[10] Lau H-K and Clerk A A 2018 Fundamental limits and non-reciprocal approaches in non-Hermitian quantum sensing *Nat. Commun.* **9** 4320
[11] Zhang M, Sweeney W, Hsu C W, Yang L, Stone A D and Jiang L 2018 Quantum noise theory of exceptional point sensors (arXiv:1805.12001[quant-ph])
[12] Wang Y-X and Clerk A A 2019 Non-Hermitian dynamics without dissipation in quantum systems *Phys. Rev.* A **99** 063834
[13] Schomerus H 2010 Quantum noise and self-sustained radiation of $\mathcal{PT}$-symmetric systems *Phys. Rev. Lett.* **104** 233601
[14] Yoo G, Sim H-S and Schomerus H 2011 Quantum noise and mode nonorthogonality in non-Hermitian $\mathcal{PT}$-symmetric optical resonators *Phys. Rev.* A **84** 063833
[15] Agarwal G S and Qu K 2012 Spontaneous generation of photons in transmission of quantum fields in $\mathcal{PT}$-symmetric optical systems *Phys. Rev.* A **85** 031802
[16] Vashahri-Ghamsari S, He B and Xiao M 2017 Continuous-variable entanglement generation using a hybrid $\mathcal{PT}$-symmetric system *Phys. Rev.* A **96** 033806
[17] Longhi S 2018 Quantum interference and exceptional points *Opt. Lett.* **43** 5371–4

[18] Vashahri-Ghamsari S, He B and Xiao M 2019 Effects of gain saturation on the quantum properties of light in a non-Hermitian gain-loss coupler *Phys. Rev.* A **99** 023819
[19] Jan P, Antonín L, Kalaga J K, Leoński W and Adam M 2019 Nonclassical light at exceptional points of a quantum $\mathcal{PT}$-symmetric two-mode system *Phys. Rev.* A **100** 053820
[20] Klauck F, Teuber L, Ornigotti M, Heinrich M, Scheel S and Alexander S 2019 Observation of *PT*-symmetric quantum interference *Nat. Photon.* **13** 883–7
[21] Naikoo J, Thapliyal K, Banerjee S and Pathak A 2019 Quantum zeno effect and nonclassicality in a $\mathcal{PT}$-symmetric system of coupled cavities *Phys. Rev.* A **99** 023820
[22] Jaramillo Á B, Ventura-Velázquez C, de J León-Montiel R, Joglekar Y N and Rodríguez-Lara B M 2020 Pt-symmetry from lindblad dynamics in a linearized optomechanical system *Sci. Rep.* **10**
[23] Zhang M, Sweeney W, Hsu C W, Yang L, Stone A D and Jiang L 2019 Quantum noise theory of exceptional point amplifying sensors *Phys. Rev. Lett.* **123** 180501
[24] Nielsen M A and Chuang I L 2010 *Quantum Computation and Quantum Information: 10th Anniversary Edition* (Cambridge: Cambridge University Press)
[25] Braunstein S L and van Loock P 2005 Quantum information with continuous variables *Rev. Mod. Phys.* **77** 513–77
[26] McDonald A, Pereg-Barnea T and Clerk A A 2018 Phase-dependent chiral transport and effective non-hermitian dynamics in a bosonic kitaev-majorana chain *Phys. Rev.* X **8** 041031
[27] Ollivier H and Zurek W H 2001 Quantum discord: a measure of the quantumness of correlations *Phys. Rev. Lett.* **88** 017901
[28] Henderson L and Vedral V 2001 Classical, quantum and total correlations *J. Phys. A: Math. Gen.* **34** 6899–905
[29] Modi K, Brodutch A, Cable H, Paterek T and Vedral V 2012 The classical-quantum boundary for correlations: discord and related measures *Rev. Mod. Phys.* **84** 1655–707
[30] Cao W, Lu X, Meng X, Sun J, Shen H and Xiao Y 2020 Reservoir-mediated quantum correlations in non-hermitian optical system *Phys. Rev. Lett.* **124** 030401
[31] Schindler J, Li A, Zheng M C, Ellis F M and Kottos T 2011 Experimental study of active lrc circuits with $\mathcal{PT}$ symmetries *Phys. Rev.* A **84** 040101
[32] Bender C M, Berntson B K, Parker D and Samuel E 2013 Observation of pt phase transition in a simple mechanical system *Am. J. Phys.* **81** 173–9
[33] Dast D, Haag D, Cartarius H and Wunner G 2014 Quantum master equation with balanced gain and loss *Phys. Rev.* A **90** 052120
[34] Longhi S 2019 Quantum statistical signature of $\mathcal{PT}$ symmetry breaking (arXiv:1912.07460)
[35] Huber J, Kirton P, Rotter S and Rabl P 2020 Emergence of pt-symmetry breaking in open quantum systems *SciPost Phys* **9** 052
[36] Gardiner C and Zoller P 2004 *Quantum Noise: A Handbook of Markovian and Non-Markovian Quantum Stochastic Methods with Applications to Quantum Optics* (*Springer Series in Synergetics*) 3rd edn (Berlin: Springer)
[37] Ferraro A, Olivares S and Paris M G A 2005 *Gaussian States in Quantum Information* (Napoli: Bibliopolis)
[38] Olivares S 2012 Quantum optics in the phase space *Eur. Phys. J. Spec. Top.* **203** 3–24
[39] Cover T M and Thomas J A 2006 *Elements of Information Theory* 2nd edn (New York: Wiley)
[40] Pirandola S, Spedalieri G, Braunstein S L, Cerf N J and Lloyd S 2014 Optimality of Gaussian discord *Phys. Rev. Lett.* **113** 140405
[41] Giorda P and Matteo G A 2010 Paris. Gaussian quantum discord *Phys. Rev. Lett.* **105** 020503
[42] Adesso G and Datta A 2010 Quantum versus classical correlations in Gaussian states *Phys. Rev. Lett.* **105** 030501
[43] Adesso G, Ragy S, Lee A R and Lee 2014 Continuous variable quantum information: Gaussian states and beyond *Open Syst. Inf. Dyn.* **21** 1440001
[44] Adesso G, Girolami D and Serafini A 2012 Measuring Gaussian quantum information and correlations using the rényi entropy of order 2 *Phys. Rev. Lett.* **109** 190502
[45] Kim M S, Son W, Bužek V and Knight P L 2002 Entanglement by a beam splitter: nonclassicality as a prerequisite for entanglement *Phys. Rev.* A **65** 032323
[46] Scheel S and Szameit A 2018 $\mathcal{PT}$-symmetric photonic quantum systems with gain and loss do not exist *Europhys. Lett.* **122** 34001
[47] Korolkova N and Leuchs G 2019 Quantum correlations in separable multi-mode states and in classically entangled light *Rep. Prog. Phys.* **82** 056001
[48] Ciccarello F and Giovannetti V 2012 Creating quantum correlations through local nonunitary memoryless channels *Phys. Rev.* A **85** 010102
[49] Hu X, Fan H, Zhou D L and Liu W-M 2012 Necessary and sufficient conditions for local creation of quantum correlation *Phys. Rev.* A **85** 032102
[50] Streltsov A, Hermann K and Bruß D 2011 Behavior of quantum correlations under local noise *Phys. Rev. Lett.* **107** 170502
[51] Ciccarello F and Giovannetti V 2012 Local-channel-induced rise of quantum correlations in continuous-variable systems *Phys. Rev.* A **85** 022108
[52] Madsen L S, Berni A, Lassen M and Andersen U L 2012 Experimental investigation of the evolution of Gaussian quantum discord in an open system *Phys. Rev. Lett.* **109** 030402
[53] Roccati F *et al* Quantum correlations dynamics in multipartite gain–loss systems (in preparation)
[54] Adesso G, Bromley T R and Cianciaruso M 2016 Measures and applications of quantum correlations *J. Phys. A: Math. Theor.* **49** 473001
[55] Streltsov A 2015 *Quantum Correlations Beyond Entanglement: And Their Role in Quantum Information Theory* (*Springer Briefs in Physics*) (Berlin: Springer)
[56] Gu M, Chrzanowski H M, Assad S M, Symul T, Modi K, Ralph T C, Vedral V and Lam P K 2012 Observing the operational significance of discord consumption *Nat. Phys.* **8** 671–5
[57] Dakic B *et al* 2012 Quantum discord as resource for remote state preparation *Nat. Phys.* **8** 666–70
[58] Piani M, Gharibian S, Adesso G, Calsamiglia J, Horodecki P and Winter A 2011 All nonclassical correlations can Be activated into distillable entanglement *Phys. Rev. Lett.* **106** 220403
[59] Adesso G, D'Ambrosio V, Nagali E, Piani M and Sciarrino F 2014 Experimental entanglement activation from discord in a programmable quantum measurement *Phys. Rev. Lett.* **112** 140501
[60] Alexander Streltsov , Hermann K and Bruß D 2011 Linking quantum discord to entanglement in a measurement *Phys. Rev. Lett.* **106** 160401
[61] Croal C, Peuntinger C, Chille V, Marquardt C, Leuchs G, Korolkova N and Mista L 2015 Entangling the whole by beam splitting a part *Phys. Rev. Lett.* **115** 190501

[62] Chuan T K, Maillard J, Modi K, Paterek T, Paternostro M and Piani M 2012 Quantum discord bounds the amount of distributed entanglement *Phys. Rev. Lett.* **109** 070501
[63] Peuntinger C, Chille V, Mišta L, Korolkova N, Förtsch M, Jan K, Marquardt C and Leuchs G 2013 Distributing entanglement with separable states *Phys. Rev. Lett.* **111** 230506
[64] Vollmer C E, Schulze D, Tobias E, Händchen V, Fiurášek J and Schnabel R 2013 Experimental entanglement distribution by separable states *Phys. Rev. Lett.* **111** 230505
[65] Fedrizzi A, Zuppardo M, Gillett G G, Broome M A, Almeida M P, Paternostro M, White A G and Paterek T 2013 Experimental distribution of entanglement with separable carriers *Phys. Rev. Lett.* **111** 230504
[66] Girolami D, Souza A M, Giovannetti V, Tufarelli T, Filgueiras J G, Sarthour R S, Soares-Pinto D O, Oliveira I S and Adesso G 2014 Quantum discord determines the interferometric power of quantum states *Phys. Rev. Lett.* **112** 210401